Short Papers

Asymptotically Stable End-Point Regulation of a Flexible SCARA/Cartesian Robot

S. S. Ge, T. H. Lee, and G. Zhu

***Abstract*—This paper presents a class of asymptotically stable end-point regulators for a flexible SCARA/Cartesian robot. Firstly, the closed-loop stability is proven for the original distributed-parameter system; then, through explicitly solving the partial differential equations (PDE's) of the system, asymptotic stability is obtained for the undamped truncated system, in which the distributed flexibility of the robot link is represented by an *arbitrary* finite number of flexible modes. The controllers possess some attractive advantages for practical applications. Computer simulations are provided to illustrate the effectiveness of the approach.**

***Index Terms*— Distributed-parameter system, flexible SCARA/Cartesian robot, regulation.**

I. Introduction

Robots with lightweight flexible links possess many advantages over the conventional rigid-link ones, such as lower arm cost, better energy efficiency, higher operation speed, and improved mobility. These advantages greatly motivate the research in modeling and control of flexible-link robots.

The SCARA/Cartesian robots are widely used in industry, especially in automatic manufacturing assembly [1]. In order to improve industrial productivity, it is very desirable to build the robot link with lightweight material and, thus, increase the payload-to-weight ratio. When such a robot is carrying a large payload and moving at a high speed, the effect of link flexibility will be nonnegligible, and the traditional collocated control, e.g., the proportional and derivative (PD) feedback is no longer sufficient for fast and accurate positioning. Due to the distributed link flexibility, the system, described by partial differential equations (PDE's), is actually a distributed-parameter system of infinite dimensions. Its nonminimum phase behavior from the base input to the end-point output makes it very difficult to achieve high-level performance and robustness simultaneously [2]. Various kinds of control techniques have been investigated to design noncollocated controllers to improve the performance of flexible robot systems. Most of these approaches are based on the truncated finite-dimensional models, for example, in [5]–[9], etc. The truncated models can be obtained by the model analysis, in which the link flexibility is represented by an infinite number of flexible modes. The finite-dimensional models are derived by truncating the infinite number of modes to a finite number, i.e., the modes with comparatively higher frequencies are neglected. Some problems associated with the truncated-model-based methods have been highlighted in the literature: 1) control and observation spillovers may occur due to the ignored high-frequency dynamics [3]; 2) computing burden will be increased when a relatively higher order controller (corresponding to the model with more flexible modes) is used to achieve higher accuracy of performance; and 3) the controllers may be difficult to implement from the engineering point of view, since full states measurements/observers are often required.

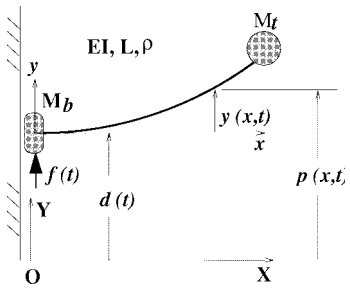

Fig. 1. The flexible SCARA/Cartesian robot.

In this paper, we present a class of asymptotically stable set-point controllers for flexible SCARA/Cartesian robots. The controllers are constructed by introducing a nonlinear vibration feedback term into the traditional collocated base PD controller. This is motivated by the fact that the link flexibility is not taken into consideration in the PD control. The vibration feedback will give explicit evaluation of link flexibility and is expected to provide direct control effort on vibration suppression. Firstly, the closed-loop stability is proven for the original distributed-parameter system. This implies that the aforementioned problems of truncated-model-based methods are avoided in the sense of achieving closed-loop stability. Then, through explicit solving of the PDE's of the system, asymptotic stability is proven for the undamped truncated system, in which the link flexibility is represented by an arbitrary finite number of flexible modes. It should be pointed out that the controllers presented in this paper are significantly different from the traditional truncated-model-based ones in the following aspects: 1) the problem of control and observation spillovers does not exist; 2) the asymptotic stability can be guaranteed for a truncated system with any finite number of flexible modes without increasing the order of the controller; and 3) the vibration feedback can be arbitrarily chosen depending on practically available sensor facilities. The controllers are also robust to parameter uncertainties, because they are independent of the system parameters. These advantages are very attractive to engineering practice. Numerical simulations are provided to show the effectiveness of the approach, in which the vibration feedback is chosen to be the base strain of the link, which can be measured by the most frequently used sensor in flexible robot control, i.e., the strain gauge.

The remainder of this paper is organized as follows. In Section II, the dynamic equations (PDE's) of the system are obtained. The controller design is presented in Section III. Computer simulations are given in Section IV, followed by the conclusion in Section V.

II. Dynamics of the System

As shown in Fig. 1, the flexible SCARA/Cartesian robot is described by a flexible manipulator with a translational base. Different from the flexible robots with *rotational* joints, which have been much studied in the literature, the vibration in this case is caused by the translational acceleration at the base, instead of the joint angular acceleration [1].

Manuscript received August 31, 1996; revised October 28, 1997. Recommended by Technical Editor H. Kazerooni.

The authors are with the Department of Electrical Engineering, National University of Singapore, Singapore 119260.

Publisher Item Identifier S 1083-4435(98)04473-1.

Suppose that the robot is operated in the horizontal plane without gravitational influence. Frame X–Y is the fixed inertia frame, and frame x-y is the local reference frame. System parameters and variables are as follows: L is the length of the link; EI is the uniform flexural rigidity; ρ is the uniform mass per unit length of the link; M_b is the mass of the translational base; M_t is the concentrated mass tip payload; $f(t)$ is the control force applied to the base; $d(t)$ is the position of the base; $y(x,t)$ is the elastic deflection measured from the undeformed link; and $p(x,t) := d(t) + y(x,t)$ is the position of the flexible link.

We make the standard assumption of small deflection. The total kinetic energy and the total potential energy of the system are given by

$$E_k = \frac{1}{2}M_b\dot{d}^2(t) + \frac{\rho}{2}\int_0^L \dot{p}^2(x,t)\,dx + \frac{1}{2}M_t\dot{p}^2(L,t) \tag{1}$$

$$E_p = \frac{EI}{2}\int_0^L [y''(x,t)]^2\,dx \tag{2}$$

where the dots and primes denote the derivatives with respect to time and space variable x, respectively. Invoking the extended Hamilton's Principle

$$\int_{t_o}^{t_f} \delta[E_k - E_p + f(t)\,d(t)]\,dt = 0 \tag{3}$$

and noting that the shear force at the base of the flexible link can be calculated by

$$EIy'''(0,t) = -\rho\int_0^L [\ddot{d}(t) + \ddot{y}(t,x)]\,dx - M_t[\ddot{d}(t) + \ddot{y}(L,t)] \tag{4}$$

we arrive at the following dynamic equations and corresponding boundary conditions:

$$M_b\ddot{d}(t) = f(t) + EIy'''(0,t) \tag{5}$$

$$\rho[\ddot{d}(t) + \ddot{y}(x,t)] = -EIy''''(x,t) \tag{6}$$

$$y(0,t) = 0, \quad y'(0,t) = 0, \quad y''(L,t) = 0 \tag{7}$$

$$EIy'''(L,t) = M_t[\ddot{d}(t) + \ddot{y}(L,t)]. \tag{8}$$

III. Asymptotically Stable End-Point Regulation

In this paper, vibration feedback is introduced into the pure base PD controller to improve the system performance. The controllers have the following general form:

$$f(t) = -k_p[d(t) - d_f] - k_v\dot{d}(t) - kg(t)\cdot\mathrm{sgn}\,(\dot{d})\int_0^t |\dot{d}(\tau)|g(\tau)\,d\tau \tag{9}$$

where k_p, k_v are the positive PD feedback gains, $k \geq 0$ is the vibration feedback gain, d_f is the set-point position of the base, $\mathrm{sgn}\,(\dot{d})$ equals -1, 0, and 1 when $\dot{d}$ is, respectively, negative, zero, and positive, and $g(t)$ is the vibration feedback. The stability of the closed-loop system is stated in the following two theorems.

Theorem 1: The controller in (9) can guarantee the closed-loop stability of the original distributed-parameter infinite-dimensional system.

Proof: See Appendix A. ∎

Theorem 2: The controller in (9) can guarantee the asymptotic stability of the undamped truncated system, which is obtained by representing the flexible deflection by an arbitrary finite number of flexible modes.

Proof: See Appendix B. ∎

Some of the attractive advantages of the controller (9) to practical engineering applications are summarized in the following remarks.

Remarks:

1) Controller (9) is very simple and easy to implement. All the control parameters are independent of system parameters and, thus, it possesses stability robustness to system parameter uncertainties. In fact, the closed-loop system is stable as long as $k_p, k_v > 0$ and $k \geq 0$. The third nonlinear term is used to evaluate and control the vibrations. The nonlinear term is introduced in an attempt to include explicit evaluation of the vibration into the controller and, thus, provide some explicit control efforts on vibration suppression. At this point, we would like to improved the control performance without destabilizing the closed-loop system. Although the pure PD controller (with $g(t) = 0$) can also stabilize the system, the control performance of a "flexible" robot system under pure PD control is very unsatisfactory, due to the vibration of the flexible link. (Note that, in regulating a "flexible"-link robot, the variable to be regulated is the position of the end effector instead of the joint angle.) Obviously, the reason is that there is no evaluation of vibration in the pure PD control and, subsequently, no explicit control effort is provided to suppress the vibration. Therefore, by introducing the nonlinear term associated with vibration, we are able to not only guarantee the stability, but also improve the system performance.
2) Theoretically, the stability of the system will not be destroyed with any $g(t)$ feedback, but it is preferable to choose $g(t)$ associated with the vibration of the flexible link. According to actually available instrumentation, $g(t)$ can be any variable or any combination of variables associated with the vibration of the flexible link. As a result, introducing $g(t)$ feedback, compared with the traditional joint PD control, allows explicit evaluation of vibration and, thus, provides explicit control effort in vibration suppression. Some examples of the vibration variables are $y(x_s,t)$ (deflection at $x = x_s$), $y'(x_s,t)$ (rotation at $x = x_s$), $y''(x_s,t)$ (strain at $x = x_s$), $y'''(x_s,t)$ (shear force at $x = x_s$). Choosing different $g(t)$'s leads to a set of controllers. Owing to the above statements, it is clear that the possible measurement noise existing in $g(t)$ feedback will not destroy the system's stability.
3) With controller (9), the drawbacks associated with truncated-model-based approaches mentioned in Section I are essentially avoided. This fact can be seen by considering system energy. Since the system is undamped, the total change in energy of the system must be equal to the work done by the control force, i.e.,

$$E_k - E_{k0} + E_p - E_{p0} = \int_0^t f(t)\dot{d}(t)\,dt \tag{10}$$

where E_{k0} and E_{p0} are the kinetic energy and the potential energy of the system at the initial moment. Differentiating with respect to time on both sides of (10) yields $\dot{E}_k + \dot{E}_p = \dot{d}(t)f(t)$, through which we can directly arrive at (19) in the proof of *Theorem 1*. This implies that the proof can be achieved without using the dynamic equations of the system. Therefore, the controller (9) can be regarded as nonmodel-based and, thus, nonmodel truncation, in the sense of achieving closed-loop stability.
4) Although model-truncation has also been invoked in proving the asymptotic stability in *Theorem 2*, controller (9) has the following significant differences from the traditional truncated-model-based ones.
   a) Since controller (9) is not of states-feedback type, reconstruction of flexible modes is not necessary and, thus,

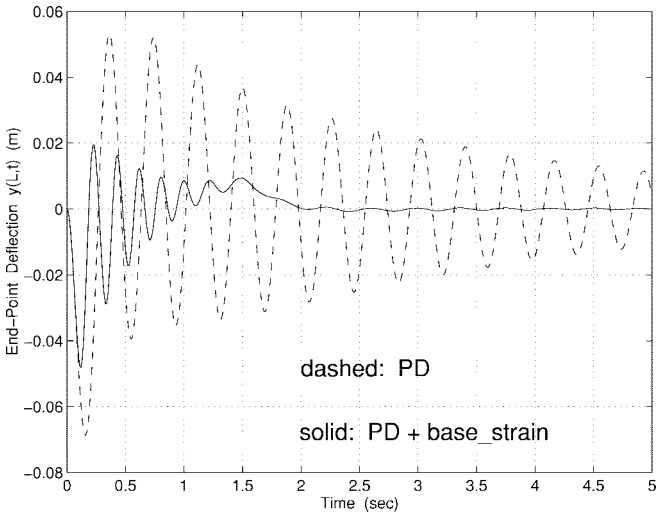

Fig. 2. End-point deflection $y(L,t)$ in unloaded case.

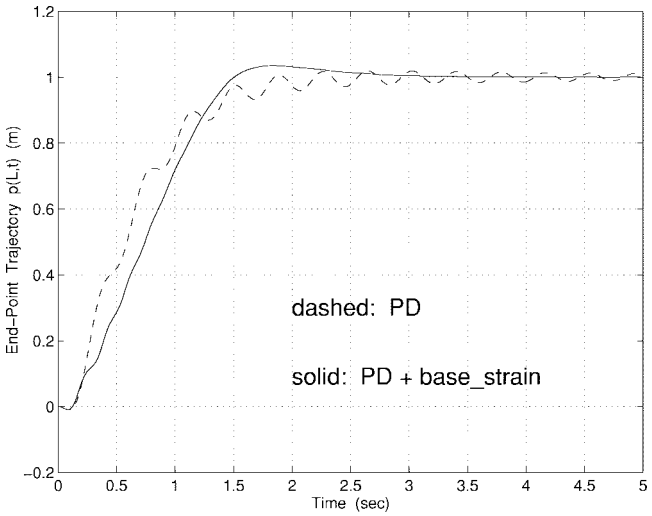

Fig. 3. End-point trajectory $p(L,t)$ in unloaded case.

the problem of control/observation spillovers, which is caused by ignoring high-frequency modes in controller and observer design, does not exist.

b) Asymptotic stability can be guaranteed for a truncated system with an *arbitrary* finite number of flexible modes (*Theorem 2*) without the need to increase the order of the controller and, thus, the computing burden can be always kept light.

c) The controller allows great freedom in feedback design and is very easy to implement, since the vibration feedback $g(t)$ can be chosen according to available sensor facilities, and no high-order signal measurements are needed.

IV. Simulation Tests

As stated in *Remark 2)*, there is no theoretical restriction on the choice of $g(t)$, but it is reasonable to choose $g(t)$ associated with vibration, in order to improve the system performance. It should be pointed out that theoretical guidelines on selecting $g(t)$ to *optimize* the performance are currently lacking. As an example, some numerical simulations are carried out below with $g(t)$ being the base-strain $y''(0,t)$ feedback, which can be easily measured by attaching a strain gauge at the base of the link.

In the simulations, the system parameters are given as $L = 1.0$ m, $EI = 2.0\,\mathrm{N}\cdot\mathrm{m}^2$, $\rho = 0.1$ kg/m, and $M_b = 0.5$ kg. The plant is simulated by a four-mode assumed-modes model and the set-point value of regulation is $d_f = 1.0$ m.

The PD feedback part of the controller is determined as follows. For the pure base PD controller

$$f_{\mathrm{PD}} = -k_p[d(t) - d_f] - k_v\dot{d}(t)$$

if the flexible link is assumed to be rigid, i.e., $y(x,t) \equiv 0$, substituting f_{PD} and (4) into (5) yields the following closed-loop base motion error equation:

$$M\ddot{e}(t) + k_v\dot{e}(t) + k_p e = 0 \tag{11}$$

where $M = M_b + \rho L + M_t$ and $e = d(t) - d_f$. Therefore, to achieve critical damping ($\xi = 1$) in base regulation, we have $k_p = M\omega_n^2$ and $k_v = 2M\omega_n$, in which ω_n is the natural frequency of the second-order equation (11).

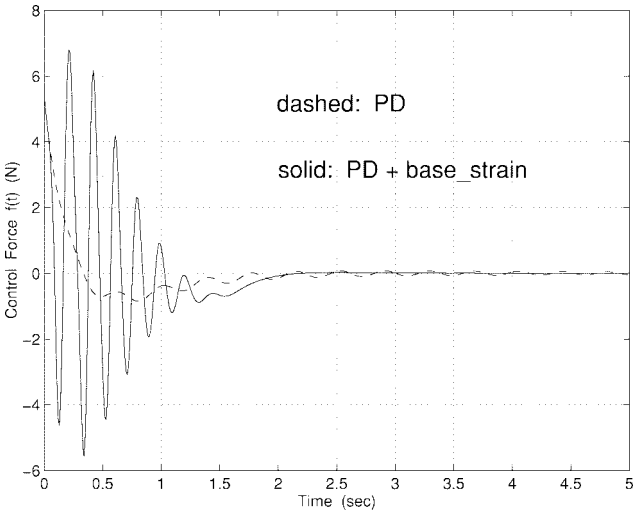

Fig. 4. Control force $f(t)$ in unloaded case.

Firstly, we consider the unloaded case, i.e., $M_t = 0$. Let $\omega_n = 3.0$; we have $k_p = 5.4$ and $k_v = 3.6$, and the controller is given by

$$f(t) = -5.4[d(t) - d_f] - 3.6\dot{d}(t) - 10\,000y''(0,t)\,\mathrm{sgn}\,(\dot{d})\int_0^t |\dot{d}(\tau)|y''(0,\tau)\,d\tau. \tag{12}$$

It should be pointed out that the feedback gain $k = 10\,000$ may not be optimal. The simulation is only given for illustrative purposes. For comparison, the performance of the pure base PD control is also plotted with dashed lines. The end-point deflection $y(L,t)$ is given in Fig. 2. It can be seen that, after introducing the base-strain feedback, the undesirable deflection converges quite quickly. This leads to a fast and oscillation-free end-point regulation performance, as shown in Fig. 3. The control force is given in Fig. 4.

Then, the loaded robot with $M_t = 0.1$ kg is simulated. In this case, $M = 0.7$ kg, and letting $\omega_n = 2.3$ leads to the following pure base PD controller:

$$f_{\mathrm{PD}} = -3.7[d(t) - d_f] - 3.2\dot{d}(t).$$

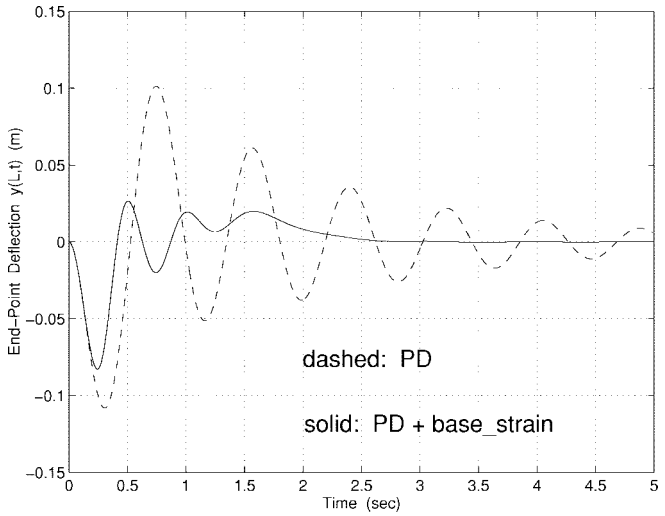

Fig. 5. End-point deflection $y(L,t)$ in loaded case.

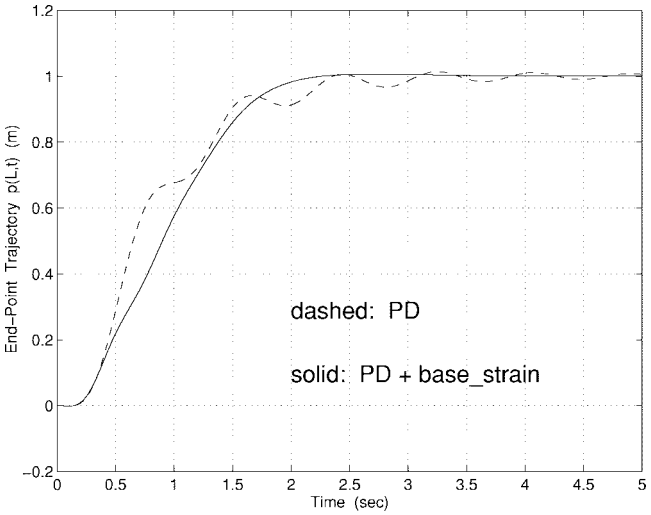

Fig. 6. End-point trajectory $p(L,t)$ in loaded case.

After introducing $g(t) = y''(0,t)$ feedback, we have

$$f(t) = -3.7[d(t) - d_f] - 3.2\dot{d}(t) - 800y''(0,t)\,\mathrm{sgn}\,|(\dot{d})\int_0^t |\dot{d}(\tau)|y''(0,\tau)\,d\tau. \tag{13}$$

Again, we note that $k = 800$ may not be the best choice. The performance of the system is shown in Figs. 5 and 6. Compared with the pure base PD control, the performance of the controller with $g(t)$ feedback exhibits much smaller vibration, and the end-point regulation has been improved greatly. The control force is shown in Fig. 7.

V. Conclusion

A class of asymptotically stable controllers has been presented for regulation of a flexible SCARA/Cartesian robot. The new controllers, which possess some attractive advantages for practical applications, are constructed by introducing a nonlinear vibration feedback term into the traditional PD controller. Numerical simulations are provided with the vibration feedback being the base strain of the flexible link, and a set of satisfactory control results are obtained.

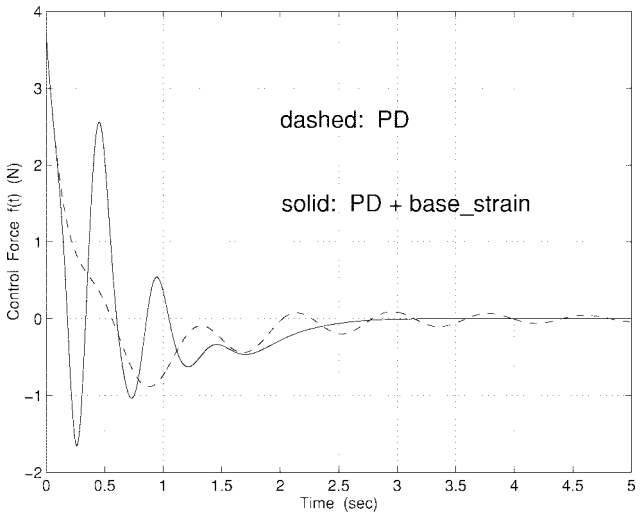

Fig. 7. Control force $f(t)$ in loaded case.

Although it is reasonable to choose $g(t)$ to be associated with vibration, we shall point out that explicit guidelines for choosing $g(t)$ to optimize the performance are currently lacking. The effect of $g(t)$ feedback on system dynamic behavior will be investigated in our future research.

Appendix A
Proof of *Theorem 1*

Consider the following Lyapunov function:

$$V(t) = E_k + E_p + \tfrac{1}{2}k_p[d(t) - d_f]^2 + \tfrac{1}{2}k\left[\int_0^t |\dot{d}(\tau)|g(\tau)\,d\tau\right]^2 \tag{14}$$

where E_k and E_p are given in (1) and (2). The time derivative of $V(t)$ is

$$\dot{V} = \dot{E}_k + \dot{E}_p + k_p\dot{d}[d(t) - d_f] + k\dot{d}g(t)\,\mathrm{sgn}\,(\dot{d}) \cdot \int_0^t |\dot{d}(\tau)|g(\tau)\,d\tau. \tag{15}$$

We assume that the deflection variable $y(x,t)$ satisfies

$$\frac{d}{dt}\int_0^L \dot{y}^2(x,t)\,dx = \int_0^L \left[\frac{d}{dt}\dot{y}^2(x,t)\right]dx. \tag{16}$$

Invoking (1) and through some simple derivations, we have

$$\dot{V}(t) = M_b\dot{d}\ddot{d} + L\rho\dot{d}\ddot{d} + \rho\dot{d}\int_0^L \ddot{y}\,dx + M_t\dot{d}(\ddot{d} + \ddot{y}_L) + \Delta + \dot{E}_p + k_p\dot{d}[d(t) - d_f] + k\dot{d}g(t) \cdot \mathrm{sgn}\,(\dot{d})\int_0^t |\dot{d}(\tau)|g(\tau)\,d\tau \tag{17}$$

where $y_L := y(L,t)$ for simplicity, and Δ is given by

$$\Delta = \rho\int_0^L \dot{y}(\ddot{d} + \ddot{y})\,dx + M_t\dot{y}_L(\ddot{d} + \ddot{y}_L).$$

From (6) and (8), and using integration by parts, Δ can be calculated as

$$\Delta = -EI\int_0^L \dot{y}y''''\,dx + EI\dot{y}_L y_L''' = EI\left[\dot{y}_L' y_L'' - \dot{y}_0' y_0'' - \int_0^L y''\dot{y}''\,dx + \dot{y}_0 y_0'''\right]$$

where $y_0 := y(0,t)$ for simplicity. Recalling the boundary conditions in (7), we further have

$$\Delta = -EI \int_0^L y'' \dot{y}'' \, dx = -\dot{E}_p. \tag{18}$$

Substituting (18) into (17) and noting (4) and (5) give

$$\dot{V} = \dot{d}(t) f(t) + k_p \dot{d}[d(t) - d_f] + k \dot{d} g(t) \operatorname{sgn}(\dot{d}) \cdot \int_0^t |\dot{d}(\tau)| g(\tau) \, d\tau. \tag{19}$$

Now, substituting (9) into (19) leads to

$$\dot{V}(t) = -k_v \dot{d}^2(t) \tag{20}$$

which is negative semidefinite. This implies that the closed-loop system is energy dissipative and, hence, stable. (QED)

Appendix B
Proof of *Theorem 2*

Using the same Lyapunov function (14), we consider the motion of the system in the largest invariant set in the set $\dot{V} = 0$. When $\dot{V} \equiv 0$, from (20), we have $\dot{d} \equiv 0$ and, subsequently, $\ddot{d} = 0$. Controller (9) becomes $f = -k_p[d - d_f]$, which is a constant. The dynamic equations and boundary conditions reduce to

$$EIy''''(0,t) - k_p[d - d_f] = 0 \tag{21}$$

$$\rho \ddot{y}(x,t) = -EIy''''(x,t) \tag{22}$$

$$y(0,t) = 0$$

$$y'(0,t) = 0$$

$$y''(L,t) = 0 \tag{23}$$

$$EIy'''(L,t) = M_t \ddot{y}(L,t). \tag{24}$$

We use the Method of Separating Variables [11] to solve (22) under conditions (23) and (24). The solution to (22) is assumed to be of the form $y(x,t) = \Phi(x)Q(t)$, and (22) becomes

$$\frac{\Phi''''}{\Phi} \cdot \frac{EI}{\rho} = -\frac{\ddot{Q}}{Q}. \tag{25}$$

Obviously, both sides of (25) must equal a constant, for example, K, and we arrive at

$$\ddot{Q}(t) + KQ(t) = 0 \tag{26}$$

$$\Phi''''(x) = \frac{\rho}{EI} K \Phi(x). \tag{27}$$

From (23) and (24), we have

$$\Phi(0) = 0, \quad \Phi'(0) = 0, \quad \Phi''(L) = 0 \tag{28}$$

$$\Phi'''(L) = -\frac{M_t}{EI} K \Phi(L). \tag{29}$$

Equation (27) and conditions (28) and (29) describe the corresponding boundary value problem, to solve which, all possible K should be considered.When $K = 0$, the solution to (27) is of the form $\Phi(x) = C_1 x^3 + C_2 x^2 + C_3 x + C_4$ and, subsequently, $C_1 = C_2 = C_3 = C_4 = 0$, which indicates trivial solution.

When $K < 0$, letting $K = -\omega^2$ with $\omega \neq 0$ (27) becomes

$$\Phi''''(x) = -\left(\frac{\beta}{L}\right)^4 \Phi(x) \tag{30}$$

where

$$\left(\frac{\beta}{L}\right)^4 = \frac{\rho}{EI}\omega^2. \tag{31}$$

The general solution to (30) is of the form

$$\Phi(x) = C_1 e^{ax} \sin(ax) + C_2 e^{ax} \cos(ax) + C_3 e^{-ax} \sin(ax) + C_4 e^{-ax} \cos(ax) \tag{32}$$

where $a = \sqrt{2}\beta/2L$. Substituting (32) into (28) and (29) leads to the following set of equations:

$$C_2 + C_4 = 0$$

$$C_1 + C_2 + C_3 - C_4 = 0$$

$$\begin{aligned}
&(C_1 e^{aL} - C_3 e^{-aL}) \cos(aL) \\
&\quad - (C_2 e^{aL} - C_4 e^{-aL}) \sin(aL) = 0 \\
&(C_1 e^{aL} + C_4 e^{-aL})[\cos(aL) - \sin(aL)] \\
&\quad - (C_2 e^{aL} - C_3 e^{-aL})[\cos(aL) + \sin(aL)] \\
&\quad - 2\frac{aM_t}{\rho}[C_1 e^{aL} \sin(aL) + C_2 e^{aL} \cos(aL) \\
&\quad + C_3 e^{-aL} \sin(aL) + C_4 e^{-aL} \cos(aL)] = 0.
\end{aligned} \tag{33}$$

The determinant of the coefficient matrix of (33), as a function of a, is given by

$$\operatorname{Det}(a) = 2\cosh(2aL) + 4\frac{aM_t}{\rho}\sinh(2aL) + 2\cos(2aL) - 4\frac{aM_t}{\rho}\sin(2aL) + 4.$$

It is easy to check that $\operatorname{Det}(a) > 0$ is true for any a. Therefore, $K < 0$ also leads to trivial solution $C_1 = C_2 = C_3 = C_4 = 0$.

The last choice is $K > 0$. Let $K = \omega^2$. Recalling (31), (27) becomes

$$\Phi''''(x) = \left(\frac{\beta}{L}\right)^4 \Phi(x). \tag{34}$$

The general solution to (34) is given by

$$\Phi(x) = C_1 \cos\frac{\beta x}{L} + C_2 \cosh\frac{\beta x}{L} + C_3 \sin\frac{\beta x}{L} + C_4 \sinh\frac{\beta x}{L}. \tag{35}$$

From (28) and (29), we have

$$\begin{aligned}
C_1 + C_2 &= 0 \\
C_3 + C_4 &= 0 \\
-C_1 \cos\beta + C_2 \cosh\beta - C_3 \sin\beta + C_4 \sinh\beta &= 0 \\
C_1\left(\sin\beta + \frac{M_t\beta}{\rho L}\cos\beta\right) + C_2\left(\sinh\beta + \frac{M_t\beta}{\rho L}\cosh\beta\right) & \\
+C_3\left(\frac{M_t\beta}{\rho L}\sin\beta - \cos\beta\right) + C_4\left(\cosh\beta + \frac{M_t\beta}{\rho L}\sinh\beta\right) &= 0.
\end{aligned} \tag{36}$$

In order to obtain nontrivial solution, the determinant of the coefficient matrix of (36) must be zero, i.e.,

$$1 + \cosh\beta\cos\beta + \frac{M_t\beta}{\rho L}(\sinh\beta\cos\beta - \cosh\beta\sin\beta) = 0 \tag{37}$$

which may be satisfied by an infinite number of β.

Once $K = \omega^2$ is decided, we obtain an infinite number of solutions to the boundary value problem [9]:

$$\phi_i(x) = A_i\left[\cosh\frac{\beta_i x}{L} - \cos\frac{\beta_i x}{L} - \gamma_i\left(\sinh\frac{\beta_i x}{L} - \sin\frac{\beta_i x}{L}\right)\right] \tag{38}$$

where

$$\gamma_i = \frac{\cosh(\beta_i) + \cos(\beta_i)}{\sinh(\beta_i) + \sin(\beta_i)}$$

with β_i are the positive solutions of (37), and A_i are nonzero constants given in [9]. The time-dependent function $Q(t)$ is now governed by

$$\ddot{Q}(t) + \omega^2 Q(t) = 0 \tag{39}$$

which indicates that $Q(t)$ is harmonic with frequency ω. For the infinite number of β_i's, we have, from (31), an infinite number of corresponding frequencies

$$\omega_i = \frac{\beta_i^2}{L^2}\sqrt{\frac{EI}{\rho}}.$$

Subsequently, an infinite number of solutions to (39) can be obtained:

$$q_i(t) = B_i \cos\omega_i t + D_i \sin\omega_i t, \qquad i = 1, 2, 3, \cdots \tag{40}$$

where B_i and D_i are constants to be determined later. Now, using the Superposition or Linearity Principle in [11], a solution of the Euler–Bernoulli's beam equation (22) can be given by

$$y(x,t) = \sum_{i=1}^{\infty} \phi_i(x) q_i(t). \tag{41}$$

Suppose a $q_i(t)$ in (41) with larger i corresponds to a mode with higher frequency. To determine B_i and D_i, we use the following orthogonal condition [9]:

$$\rho \int_0^L \phi_i \phi_j \, dx + M_t \phi_i(L)\phi_j(L) = \begin{cases} 0 & i \neq j \\ \rho & i = j. \end{cases} \tag{42}$$

Letting $y_0(x, t_0)$ and $\dot{y}_0(x, t_0)$ denote the "initial" deflection and velocity profiles of the flexible link (note that, since we are considering the motion of the system in the largest invariant set in the set $\dot{V} = 0$, the "initial" moment t_0 should denote the moment when the system motion enters the invariant set, instead of the initial operating moment), we have

$$y_0(x,t_0) = \sum_{i=1}^{\infty} \phi_i(x)(B_i \cos\omega_i t_0 + D_i \sin\omega_i t_0) \tag{43}$$

$$\dot{y}_0(x,t_0) = \sum_{i=1}^{\infty} \phi_i(x)(-B_i \sin\omega_i t_0 + D_i \cos\omega_i t_0)\omega_i. \tag{44}$$

Define

$$I_{j,1} := \int_0^L y_0(x,t_0)\phi_j(x)\,dx + \frac{M_t}{\rho} y_0(L,t_0)\phi_j(L)$$

$$I_{j,2} := \frac{1}{\omega_j}\left[\int_0^L \dot{y}_0(x,t_0)\phi_j(x)\,dx + \frac{M_t}{\rho}\dot{y}_0(L,t_0)\phi_j(L)\right].$$

From the Expansion Theorem in [12], we know that the infinite summation in (41) is *absolutely and uniformly convergent*. This implies that, if we substitute (43) and (44) into $I_{j,1}$ and $I_{j,2}$, the corresponding integrals can be calculated termwise, i.e.,

$$I_{j,1} = \sum_{i=1}^{\infty}(B_i \cos\omega_i t_0 + D_i \sin\omega_i t_0) \cdot \left[\int_0^L \phi_i(x)\phi_j(x)\,dx + \frac{M_t}{\rho}\phi_i(L)\phi_j(L)\right]$$

$$I_{j,2} = \sum_{i=1}^{\infty}\frac{\omega_i}{\omega_j}(-B_i \sin\omega_i t_0 + D_i \cos\omega_i t_0) \cdot \left[\int_0^L \phi_i(x)\phi_j(x)\,dx + \frac{M_t}{\rho}\phi_i(L)\phi_j(L)\right].$$

By invoking the orthogonal condition (42), we have

$$I_{j,1} = B_j \cos\omega_j t_0 + D_j \sin\omega_j t_0$$

$$I_{j,2} = -B_j \sin\omega_j t_0 + D_j \cos\omega_j t_0.$$

Thus, the coefficients are determined by

$$B_i = I_{i,1}\cos\omega_i t_0 - I_{i,2}\sin\omega_i t_0$$

$$D_i = I_{i,1}\sin\omega_i t_0 + I_{i,2}\cos\omega_i t_0$$

in which the subscripts j have been replaced by i to keep symbolic compatibility with (40). From Modal Analysis, those modes with comparatively low frequencies are dominant and, thus, we have the following reasonable approximation:

$$y(x,t) = \sum_{i=1}^{N} \phi_i(x) q_i(t) \tag{45}$$

where N is the number of flexible modes we use to approximate the deflection. Substituting (45) into (21) gives

$$\sum_{i=0}^{N} \alpha_i q_i(t) = 0 \tag{46}$$

where

$$\alpha_0 = 1, \quad q_0 = k_p[d_f - d]$$

$$\alpha_i = EI\phi_i''(0) = 2\frac{A_i\beta_i^2}{L^2} \neq 0.$$

Note that q_0 is a constant. For the summation in (46), it is easy to check that the inner product defined in [4, Proposition A.3, p. 987] is applicable:

$$\langle q_i, q_j\rangle := \lim_{T\to\infty}\frac{1}{T}\int_0^T q_i(t)q_j(t)\,dt = \begin{cases} = 0, & i \neq j \\ \neq 0, & i = j. \end{cases}$$

Applying this to the summation in (46) leads to the fact that each q_i $(i = 0, 1, \cdots, N)$ must be zero and, subsequently, $d = d_f$ and $y(x,t) = 0$. This implies that the truncated system is at the final equilibrium position, i.e., the final position is the largest invariant set in the set $\dot{V} = 0$. Invoking the LaSalle's Theorem, the base motion $d(t)$ and the N flexible modes of the truncated system are asymptotically stable with respect to the final position. Q.E.D.

REFERENCES

[1] Z. H. Luo, N. Kitamura, and B. Z. Guo, "Shear force feedback control of flexible robot arms," *IEEE Trans. Robot. Automat.*, vol. 11, pp. 760–765, Oct. 1995.

[2] V. A. Spector and H. Flashner, "Modeling and design implications of noncollocated control in flexible systems," *ASME J. Dyn. Syst., Meas., Contr.*, vol. 112, no. 2, pp. 186–193, June 1990.

[3] Z. H. Luo, "Direct strain feedback control of flexible robot arms: New theoretical and experimental results," *IEEE Trans. Automat. Contr.*, vol. 38, pp. 1610–1622, Nov. 1993.

[4] J. J. Shifman, "Lyapunov functions and the control of the Euler-Bernoulli beam," *Int. J. Control*, vol. 57, no. 4, pp. 971–990, 1993.

[5] B. Siciliano and W. J. Book. "A singular perturbation approach to control of lightweight flexible manipulators," *Int. J. Robot. Res.*, vol. 7, no. 4, pp. 79–90, 1988.

[6] B. Yuan, W. J. Book, and B. Siciliano, "Direct adaptive control of a one-link flexible arm with tracking," *J. Robot. Syst.*, vol. 6, no. 6, pp. 663–680, 1989.

[7] S. Q. Zhu, S. Commuri, and F. L. Lewis, "A singular perturbation approach to stabilization of the internal dynamics of multilink flexible robots," in *Proc. American Control Conf.*, 1994, vol. 2, pp. 1386–1390.

[8] R. H. Cannon, Jr. and E. Schmitz, "Initial experiments on the end-point control of a flexible one-link robot," *Int. J. Robot. Res.*, vol. 3, no. 3, pp. 62–75, 1984.

[9] Y. Sakawa, F. Matsuno, and S. Fukushima, "Modeling and feedback control of a flexible arm," *J. Robot. Syst.*, vol. 2, no. 4, pp. 453–472, 1985.

[10] H. K. Khalil, *Nonlinear Systems*. New York: Macmillan, 1992.
[11] E. Kreyszig, *Advanced Engineering Mathematics*, 7th ed. New York: Wiley, 1993, ch. 11.
[12] L. Meirovitch, *Elements of Vibration Analysis*. New York: McGraw-Hill, 1975, ch. 5, p. 218.

Design of Mechatronic Systems with Aliased Plant Modes

Jay R. Sims, Alan N. Durney, and Craig C. Smith

***Abstract*—When digital components are combined with analog systems, frequency components in the analog system which are above one-half the sampling frequency are excited by the output of digital-to-analog (D/A) converters and aliased to lower frequencies in analog-to-digital (A/D) conversion. Since low-frequency components in a digital signal excite only higher frequencies during D/A conversion which are aliased to the same lower frequencies during A/D conversion, the D/A converter, analog plant, and A/D converter can be modeled by an aliased frequency response function (AFRF) which includes these aliased frequency effects. System identification using digital excitation and acquisition can identify the AFRF directly, or it can be developed from the frequency response function of the analog plant. Using this AFRF, controller design can proceed using conventional methods, and issues of stability, controllability of aliased modes, etc., are automatically taken into account in the design process.**

***Index Terms*—Aliasing, computation delay, computer control, mechatronic systems.**

I. Introduction

Because of the great flexibility provided by digital control, analog controllers are being increasingly replaced by digital controllers [1]. However, the bulk of the systems (plants) which are controlled are still analog, making analog-to-digital (A/D) and digital-to-analog (D/A) conversion an integral part of modern control systems.

In sampling a continuous analog signal to obtain a digital representative, information containing the value of the signal between samples is lost. This loss of information is significant when the signal has frequency content above one-half the sampling frequency. Frequency components above this Nyquist frequency are aliased to lower frequencies and become indistinguishable from lower frequency components. The classical solution to this problem has been to introduce a low-pass filter, either after the D/A converter or before the A/D converter. In control systems, this approach may be inadequate for at least the following two situations.

1) Control systems may use sensors and/or actuators that combine A/D or D/A conversion with their sensing or actuating function, making filtering impossible.
2) Filtering of modes that have significant frequency content above the Nyquist frequency renders those modes either uncontrollable or unobservable.

Yang and Hu [2] investigated the controllability of aliased modes and showed that aliased modes can be stabilized. In this paper, we present the aliased frequency response function (AFRF) as a design tool for control systems with both digital and analog components. The combined digital–analog system represented by the AFRF is linear if the embedded analog system is linear. The aliasing effect included in the AFRF is sampling-frequency dependent. Additionally, the sensors and actuators used for control can also be used for system identification to identify the AFRF directly [3]. In this case, high-frequency aliased modes will appear as low-frequency modes to the controller, and system identification will identify the modes as the controller "sees" them and as represented in the AFRF.

Manuscript received July 22, 1996; revised December 23, 1997. Recommended by Technical Editor H. Kazerooni.

The authors are with the Department of Mechanical Engineering, Brigham Young University, Provo, UT 84602 USA.

Publisher Item Identifier S 1083-4435(98)04475-5.

II. Aliased Frequency Response Functions

A digital signal will have a frequency-domain representation that is periodic. Further, the negative frequency components of all signals are complex conjugates of their corresponding positive frequency counterparts. Thus, the frequency representation of a signal $i(kT), I_a(f)$ will have the properties

$$I_a(f \pm nf_s) = I_d(f) \quad I_a(nf_s - f) = I_a^*(f) \tag{1}$$

where f_s is the sampling frequency and n is any integer.

If an analog plant with a linear frequency response function $G(f)$ is stimulated by a digital input $I_a(f)$, the response $O(f) = G(f)I_a(f)$ is nonperiodic in frequency. If $O(f)$ is sampled, resulting in $O_a(f)$, aliasing causes $O_a(f)$ to have the properties attributed to I_a in [1], and $O_a(f) = I_a(f)G_a(f)$ where

$$G_a(f) = G(f) + \sum_{n-1}^{\infty} G^*(nf_s - f) + G(nf_s + f). \tag{2}$$

We see from (2) that the response of the plant at a given frequency f is the sum of its primary band response, plus the aliased components from all of its higher frequency counterparts. $G_a(f)$, the ratio of the digital (sampled) output to the digital input, is the *AFRF* and has the same properties as the digital signal I_a in (1). It can be measured using conventional digital system identification techniques, where the input and output are digital signals, or it can be obtained mathematically from the analog transfer function $G(f)$, if known. Note that $G(f)$ must include the effects of a zero-order hold if used in D/A conversion of the system inputs and, also, any computational delay that is present, since input and output samples are assumed simultaneous in the model. If the analog system to be controlled has frequency response function $H(f)$, the D/A uses a zero-order hold, and there is a delay of τ between the corresponding output (feedback) and input (control) signals:

$$G(f) = H(f)\frac{1}{f_s}\,\frac{\sin \pi(f/f_s)}{\pi(f/f_s)} e^{-j\pi(f/f_s)} e^{-jb2\pi(f/f_s)} \tag{3}$$

where b is the delay normalized to the sample period (τ/T). Computationally, it is convenient to use the z-transform formulation rather than (3) and (2), since it avoids the infinite summation:

$$G_a(f) = (1 - z^{-1})Z\left(\frac{H(s)e^{-\tau s}}{s}\right) \tag{4}$$

where

$$z = e^{j2\pi f/f_s}. \tag{5}$$